PCCP

Accepted Manuscript

ROYAL SOCIETY OF CHEMISTRY

www.rsc.org/pccp

PCCP

ARTICLE

Growth behavior of gold nanoparticles synthesized in unsaturated fatty acids by vacuum evaporation methods

Received 00th January 20xx,
Accepted 00th January 20xx

DOI: 10.1039/x0xx00000x

www.rsc.org/pccp

Akito Fujita, Yusuke Matsumoto, Mitsuaki Takeuchi,* Hiromichi Ryuto and Gikan H. Takaoka

Physical vapor evaporation of metals on low vapor pressure liquids is a simple and clean method to synthesize nanoparticles and thin films, though only little work has been conducted so far. Here, gold nanoparticles were synthesized by vacuum evaporation (VE) methods on ricinoleic acid and oleic acid, two typical unsaturated fatty acids (UFAs). The two solvents formed black aggregates after deposition and then shrunk and finally disappeared with time progress. By transmission electron microscopy (TEM) pictures, nanoparticles in ricinoleic acids formed aggregates and then dispersed by time while in oleic acid, big aggregates were not observed in all time scales. From TEM pictures and small angle X-ray scattering (SAXS) measurements, the mean size of the nanoparticles were about 4 nm in both ricinoleic and oleic acids. UV-Vis spectra were also taken as a function of time and consistent results of the growth mechanism deducted from TEM pictures were obtained. Air exposure had an influence on the behavior of the sample triggering the nanoparticle formation in both solvents. From control experiments, oxygen gas is accused of triggering the phenomenon and nanoparticles function as a catalysis for the oxidation of the UFAs. It stimulates the phenomenon and in ricinoleic acid, specifically, electrons are transferred from riconleic acid to the gold nanoparticles, enhancing the surface potential of the nanoparticles and the repulsive force between their electronic double layers.

Introduction

Metal nanoparticles are known to show novel properties compared to bulk states. The quantum size effect, high ratio of surface atoms, modulation of electronic states, etc. contribute to unique phenomenon and properties such as surface plasmon resonance (SPR),[1] catalyst effects[2] and even ferromagnetism.[3,4] In particular, gold nanoparticles are attracting much attention for applications such as bio-imagining,[5,6] drug-delivery,[5,7] environmental catalysis[2,8] and high-density data storage media.[3,4] In 2006, Torimoto *et al.*, developed a novel method to synthesize nanoparticles by acting a sputter deposition of gold onto ionic liquids (ILs).[9] This is a simple and also "clean" method to synthesize nanoparticles, where the IL functions as a stabilizer as well as a solvent. This method excludes the usage of reducing agents and stabilizers, which are indispensable in conventional "wet" chemical methods[10] causing unintentional chemical reactions[11,12] or ill their useful properties such as their catalytic effects.[13] For these purposes, much research has been conducted on "dry" synthesis methods for example, sputter deposition,[9,11,14-18] vacuum evaporation (VE)[13,19,20] and laser ablation.[12,21]

Recently, the sputter deposition method has been applied to other non-volatile liquids such as vegetable oils (composed of fatty acids)[22,23] and polyethylene glycol[24] to obtain nanoparticles. These liquids are not only bio and environmentally friendly but they are also cost effective compared to ILs, so they should be a promising candidate in industrial uses. In sputter deposition methods, however, the plasma or sputtered atoms could cause decomposition of the solvent.[18] In our preliminary experiments, when we sputtered gold to an IL (1-buthyl-3-methyl-imidazolium hexafluoro-phosphate : BMIM-PF_6), nanoparticles were synthesized but also an unusual smell occurred from the apparatus, which implies the decomposition of the IL by plasma. Indeed, the sputter deposition method can be applied to various metals for nanoparticle synthesis,[25,26] which should be a huge advantage in means of application, including high-melting-point metals which are impossible to evaporate in VE methods. However, the plasma itself can affect the growth scheme. To prevent such events, Richter conducted VE on ILs and synthesized nanoparticles.[13,18] They carried out the VE inside a rotating glass flask where the IL was applied on the flask but the mechanical disturbance induced by rotation should have an influence on the growth mechanism. Other reports demonstrating VE methods also induce some kind of mechanical disturbance to the solvent,[20] which motivated us to conduct VE on "static" solvents, where only few reports have been made.[27]

Department of Electronic Science and Engineering, Kyoto University, Kyoto 615-8510, Japan

Electronic Supplementary Information (ESI) available: This section includes details of the SAXS measurement and analysis, photographs of the sample as a function of time, TEM pictures of lattice planes observed in oleic acid, photographs of the sample exposed in different atmosphere and XPS spectra of the gold nanoparticles. See DOI: 10.1039/x0xx00000x

In this paper, we investigated VE on "static" ricinoleic acid and oleic acid, which are UFAs. Carboxyl acids act as surfactants and have been used as stabilizers of nanoparticles.[28-30] To take full advantage of the VE method, i.e. to avoid mechanical disturbance to the sample, we developed a down deposition VE apparatus. As a result, we obtained black aggregates just after deposition and found that nanoparticle formation occurs while the aggregates shrink and disappear. The phenomenon was researched by transmission electron microscopy (TEM), small-angle X-ray scattering (SAXS) and UV-Vis measurements and found a consistent result that the nanoparticles transferred from an aggregate to individual dispersed nanoparticles. We also found that the phenomenon was triggered by the exposure of oxygen, instead of mere time progress in vacuum and confirmed the oxidation of the gold atoms were negligible by X-ray photoelectron spectroscopy (XPS). We have suggested a growth mechanism which doesn't contradict with these bizarre results and VE methods should be a promising candidate for applications.

Experimental

Gold nanoparticles were synthesized by the VE method on UFAs. Fig. 1(a) shows the VE experimental apparatus used in this paper. Ricinoleic acid (purity 88.8%) and oleic acid (purity 71.6%) were purchased from Wako Pure Chemical Industries and were used as received. Fig. 1(b) and (c) shows the structural formula of ricinoleic and oleic acid, respectively. 1.0 ml of each solvent was transferred to a petri dish (diameter 36 mm) using a micropipette and the dishes were placed 10 cm below the filament and vacuumed in the apparatus. Au wires with a diameter of 0.5 mm (purity 99.99%) were purchased from Nilaco Corporation as the deposition source, and were hooked on a filament made from a W wire with a diameter of 0.8 mm (purity 99.99%, also purchased from Nilaco Corporation). The filament was heated by applying electrical current from an external power source. The deposition was conducted under a vacuum of 6×10^{-6} Torr to prevent excessive evaporation. The deposition rate was controlled to 1.0 Å/s and a total of 187Å were deposited, both were monitored by an ULVAC CRTM-1000 quartz resonator. The concentration of the gold atoms of the sample was 0.01wt%. After the deposition, the samples were taken out from the apparatus and were kept in atmospheric air until the solvent obtained a homogenous color (typically several days for ricinoleic acid and one day for oleic acid) and were then transferred to a snap vial. The nanoparticles were stable in both solvents for more than months.

TEM pictures were taken by a JEOL JEM-2200FS apparatus operating on an acceleration voltage of 200 kV. Gold nanoparticles were observed by casting the solvent on a copper grid covered with amorphous carbon and were then washed by casting isopropanol on the gird and dried. The sample were cast on the grid for 8 to 10 minutes in order to obtain a clear picture with enough particles to derive a size distribution. The washing and drying sequence was repeated several times to obtain a clear TEM picture. Size distributions were analysed using a free software ImageJ,[31] counting more than at least 900 particles for one plot. Several TEM pictures taken from different parts of the grid were used to obtain the size distribution.

SAXS measurements were taken by a RIGAKU Nano-viewer apparatus. The X-ray wavelengths were λ = 1.54 Å. The camera length was set to 1300 mm and the range of the measurement taken place was $0.14 < q < 3.2$ nm^{-1}, where $q = \frac{4\pi\sin(\theta)}{\lambda}$, q is the scattering vector, and 2ϑ is the scattering angle. Samples were measured in a handmade holder, using a 0.5 mm thick copper plate with a "U" shape cut off. Polyether Imide films (MITSUBISHI PLASTIC Superio UT Ftype) were glued on both surfaces of the copper plates to hold the sample. The holders were dried for at least a day in order to make sure the glue doesn't react with the sample. SAXS analysis were performed as previously reported from Hatakeyama *et al.*[32] Scattering profiles were obtained by the free software Fit2D.[33] Experimental data were fitted using a RIGAKU Nano-Solver software. The SAXS measurements were conducted on the samples used for TEM observation and were demonstrated after the last TEM observations were carried out. Scattering profiles and more details about SAXS measurements are shown in the ESI.

UV-Vis absorbance spectra were obtained by a Shimadzu UV-2600 apparatus. The samples were measured in a glass cell with an optical length of 10 mm in transmission mode using ricinoleic or oleic acid as a reference.

Results and Discussion

Fig. 2 shows a photograph of the fatty acids taken 5 minutes after VE deposition and when the samples had a homogenous color. We found that the behavior of the sample just after the deposition was different among the two solvents. In ricinoleic acid, black aggregates can be seen inside and on the surface of the solvent. The number of aggregates increased until one hour after deposition and then started to dissolve into the solvent, showing a dark red color at the same time. The change of color of the solvent is due to the SPR of the nanoparticle[1] indicating the emergence of nanoparticles in the range of 2-100 nm were formed while the aggregates dissolved into the solvent. The aggregates continued to dissolve with time and turned into a homogenous red or purple color after one week of deposition. In oleic acid, black aggregates formed on the surface of the solvent as like in ricinoleic acid. Also, the solvent partially presented a brown color indicating nanoparticle formation has already occurred. As like ricinoleic acid, the aggregates shrunk with time and disappeared after one day of deposition. The samples are stable for more than months in atmospheric air and were resistant to water, a huge advantage compared to nanoparticles synthesized in ILs.[34] Further details about the property of time progress will be shown in Fig. S2 of the ESI.

From visual observation, nanoparticles seemed to form aggregates and then looked to dissolve inside the solvent. This is quite a surprising phenomenon since nanoparticles usually aggregate to lower the total surface energy. We investigated

the phenomenon in more detail by taking TEM pictures by a function of time. Fig. 3 and 4 shows the TEM pictures taken after the deposition and size distributions derived from the pictures of ricinoleic and oleic acid, respectively. The time represents when the TEM grid was fabricated after the deposition. We assumed that the gold nanoparticles held on the amorphous carbon of the TEM grid are restricted from further growth (especially the growth of large aggregates). We can't deny the possibility of growth of the small individual nanoparticles in the size of few nanometers. Also, TEM observations only investigate a small part of the entire sample, so consistent results are needed from other measurements (SAXS and UV-Vis). In ricinoleic acid, aggregates in the size of several microns were observed 30 minutes after deposition. The aggregates were composed of spherical particles in the size of several nanometers and were partially coalesced which are shown in Fig. 3(b). We couldn't obtain a size distribution for the 30 minute sample from the TEM pictures, since only a few number of particles were observed away from the aggregate. However, the size scale of the particles composing the aggregate agree with the mean size estimated from TEM and SAXS measurements for 1 week samples (shown afterwards). This implies that nanoparticles are formed and finished growth within 30 minutes after deposition. This is a remarkable difference from gold nanoparticles synthesized by sputter deposition on ILs, where nanoparticle formation occurred for several hours to days.[15] For the 4 hours and 1 week samples shown in Fig. 3(c) and (d), the aggregates became smaller and the nanoparticles became more dispersed. This behavior is consistent with the visual observation where the aggregates looked blur and where a dark red color appeared. The average particle size was 3.8 nm after 4 hours and 4.5 nm after 1 week. The size distribution derived from Fig. 3(f) matched well with the SAXS measurements plotted as a red line in the same graph. On the other hand, in oleic acids, nanoparticles were mostly dispersed throughout the growth stage and only a few number of aggregates were found from the TEM pictures. The size distribution estimated from TEM pictures showed the mean size slightly decreased with time. However, the size distribution of nanoparticles in oleic acids are wider than those in ricinoleic acids. This indicates that nanoparticles in oleic acid, at least, hardly grew up after they were formed shortly after air exposure. The sized distribution obtained from Fig. 4(f) agree with the SAXS measurements.

In oleic acid, aggregates surrounded with a contrast different from the background were found (Fig. S3 of the ESI). In higher magnifications, lattice planes could be observed and were confirmed by the diffraction spots in the fast Fourier transformation. Since the lattice planes are transparent as the surrounding background, the lattice planes should indicate thin films of gold with only a few atomic layers. Thus, considering that small nanoparticles are found near the lattice planes, the thin films are residues of the aggregates formed on the surface of the solvent, just after deposition. This results suggests that the black aggregates visually observed on the surface of the solvent are actually thin films. The thin films were first formed on the surface of the solvent, then diffused into the solvent and turned into nanoparticles. These lattice planes were also observed on ricinoleic acid, which agree with the visual appearance of aggregates on the surface of ricinoleic acid, so that some of the gold atoms formed crystalline films although most of them diffused into the solvent. As mentioned before, it is crucial to gain a consistent result from other methods because we can only obtain a micro view of the sample through TEM observations. Thus, UV-Vis measurements were carried out on the samples after deposition as a function of time.

Fig. 5 shows the UV-Vis spectra of both solvents as a function of time. In ricinoleic acid, a broad peak around 600 nm can be observed 30 minutes after deposition. Dispersed gold nanoparticles are known to show a characteristic SPR peak at around 500-550 nm. The peak shift to longer wavelengths (red shift) and broadening of the peak are characteristic features of aggregation.[19] After 1 day, the peak shifts back to around 520 nm and then show a more pronounced peak corresponding to the continuous formation of the nanoparticles. The spectra resemble those of dispersed gold nanoparticles and agree well with the TEM pictures showing that the aggregates shrink in time and the nanoparticles become dispersed. In oleic acid on the other hand, the sample did not show a clear SPR peak 30 minutes after deposition. This supports the results of visual observation that revealed thin film formation on oleic acid. The SPR peak appears 4 hours after deposition and does not show a significant change after 1 day of deposition. This means that the thin films diffuse into the solvent and transfer to nanoparticles, and the phenomenon is mainly finished within 1 day. Again the spectra agree well with the TEM observations. Hence, the microscopic view of the growth scheme can be applied to the whole sample.

Evidence of a growth phase on the surface questions us whether the deposition rate has an impact on the growth scheme. According to the classical nucleation theory, the gold atoms deposited on the surface migrate around and collide with each other, forming an embryo. While most of the embryos fall apart due to their unstableness, some of them continue to grow and form a nucleus. So, the deposition rate should have a critical impact since it should enhance the frequency of collisions and formation of the nucleus. Fig. 6 shows the size distribution obtained by SAXS measurements where the VE was carried out on several deposition rates (scattering profiles are shown in Fig. S1 in the ESI). Against our expectations, we could not see a clear correlation with the size distribution and deposition rate. The mean size were around 4 nm in both solvents. A clear correlation was not observed between the size distribution and the deposition rate, so instead of the kinetic energy of the evaporated gold atoms, the interaction between the solvent and gold nanoparticle plays a decisive role in the formation of gold nanoparticles.

The difference between aggregation and thin film formation are consistent with earlier reports. Wender *et al.* sputtered silver onto vegetable oils like castor and canola oil.[23] Nanoparticle synthesis were observed in castor oil while thin film formation occurred in canola oil when the acceleration

voltage were low. They concluded that the composition of the fatty acid decided the behavior of the growth scheme: castor oil is mainly composed of ricinoleic acid (87%) which possess hydroxyl groups while canola oil is composed of oleic and linoleic acid (oleic acid 48%, linoleic acid 32%) where there are no additional function groups. They suggested that the hydroxyl groups strongly interact with the gold atoms limiting their migration, resulting in the formation of nanoparticles while there were no such strong interactions in canola oil compositions and atoms diffused on the oil surface to form thin films. A recent report also pointed out the strong interaction between gold atoms and hydroxyl group functionalized ILs.[17] ILs with hydroxyl groups confined the gold atoms on the surface of the IL and nanoparticle formation occurred on the surface. Although the two reports show different results where the nanoparticles are formed, they both suggest the strong interaction between hydroxyl groups and gold atoms. Our results show the same trend and actually verifies Wender's report. Further research on the structure of the vacuum/liquid interface needs to be conducted in order to elucidate the difference of the growth scheme in ricinoleic and oleic acid.

We also found that exposing the sample to air triggers the dispersion or formation of the nanoparticles in the UFAs as shown in Fig. S4 of the ESI. We confirmed this phenomenon by leaving the sample in vacuum (under 0.05 Torr) for a day and then exposed to the atmosphere. Black aggregates remained in both solvents and the color change occurred after the sample was exposed to air, indicating that mere time progress did not trigger the phenomenon. We therefore conducted two control experiments to identify the cause, by venting the apparatus with N_2 and a mixed gas of O_2 + He (O_2 : He = 7:3) and left it for a day. When venting the sample with N_2 gas, black aggregates remained and no color change was observed in both solvents. When venting with O_2 mixed gas, however, the aggregates disappeared and the color change was appreciated, showing that oxygen triggers the dispersion of nanoparticles. The oxidation of gold nanoparticles were negligible from the XPS spectra (shown in the ESI). UFAs are known to be unstable and easily get oxidized. Hence, the oxidization of the UFAs should have triggered the phenomenon.

Finally, we will discuss why the aggregates formed in the solvent disperse after oxygen exposure. Although aggregates in the size of microns were most observed in ricinoleic acid and lattice planes in oleic acid, counter-examples were also found. A schematic illustration of the phenomenon is shown in Fig. 7. The stability of colloids are usually described by the DLVO theory, taking into account the attractive van der Waals force and the repulsive force between the surface potentials of the colloids.[35,36] Therefore, the transition from an aggregate to a disperse state should be due to an increase in the surface potential of the nanoparticles. We've shown that the sample are sensitive to oxygen which triggers the phenomenon, letting us assume that the oxidation of the ricinoleic acid stimulates the transition. Gold nanoparticles are a famous catalysis for oxidizing organic materials and they get redox when the reaction occurs. As a result, electrons are transferred from the ricinoleic acid to the gold nanoparticles.[37] Novo *et al.*, reported the electron transfer from ascorbic acid to gold nanocrystals resulting from the oxidation of ascorbic acid.[38] We believe the same phenomenon occurred in our experiments, where electrons transferred from the ricinoleic acid to the gold nanoparticles, resulting in an increase in the surface potential.[39] Nanoparticles positioned on the surface of the aggregates get charged and break away. Thus, the aggregates shrink and finally become individual particles or very small aggregates.

In oleic acid, thin films formed on the surface of the solvent and diffused inside (induced by the oxygen exposure) which transferred into nanoparticles. We believe the surface structure again plays a role in this scheme. As mentioned before, the double bond of the UFAs are known to be unstable and easily oxidized. The oxidation of the double bond induced the diffusion of the thin films to diffuse inside the solvent. It is hard to say precisely what triggered the diffusion but the correlation can be seen by the fact that thin film formation was hardly seen when we used "old" oleic acids (about a year from the first time used), where more double bonds should be oxidized, prior to use. The thin films in the solvent should transfer into nanoparticles to decrease the total surface energy, which is higher in a 2D film than a sphere. Thus, the oxidation of the solvent induced the transfer from thin films to nanoparticles.

Conclusions

Gold nanoparticles were synthesized by VE methods on ricinoleic acid and oleic acid. From TEM pictures, gold nanoparticles first formed aggregates in ricinoleic acid and then shrunk by time, forming individual nanoparticles. In oleic acid, the nanoparticles were in a dispersed state. Lattice planes were observed in both UFAs, which were residues of the thin films formed on the surface of the solvents, which is evidence of a growth stage on the surface in VE methods. UV-Vis spectra confirmed the behavior observed in TEM pictures. The difference of the behaviors of ricinoleic and oleic acid are consistent with prior research and suggests that the structure of the vacuum/liquid interface has a strong impact on the growth scheme. Oxygen triggers the phenomenon above by oxidizing the solvent and was confirmed by XPS measurements which ruled out the possibility of the oxidation of surface gold atoms. The samples were resistive to water and were stable for more than months. Thus, the VE method should be a promising candidate for industrial applications.

Acknowledgements

The authors thank Prof. Kurata and Mr. Kiyomura for TEM observations supported by Kyoto University Nano Technology Hub in "Nanotechnology Platform Project" and Dr. Murakami for XPS measurements both sponsored by the Ministry of Education, Culture, Sports, Science and Technology (MEXT),

Japan. The authors also thank Dr. Takenaka and Dr. Saijyo for technical support on SAXS measurements.

References

1 S. K. Ghosh and T. Pal, *Chem. Rev.*, 2007, **107**, 4797-4862.
2 A. Corma and H. Garcia, *Chem. Soc. Rev.*, 2008, **37**, 2096-2126.
3 Y. Yamamoto, T. Miura, M. Suzuki, N. Kawamura, H. Miyagawa, T. Nakamura, K. Kobayashi, T. Teranishi and H. Hori, *Phys. Rev. Lett.*, 2004, **93**, 116801.
4 R. Gréget, G. L. Nealon, B. Vileno, P. Turek, C. Mény, F. Ott, A. Derory, E. Voirin, E. Rivière, A. Rogalev, F. Wilhelm, L. Joly, W. Knafo, G. Ballon, E. Terazzi, J.-P. Kappler, B. Donnio and J.-L. Gallani, *ChemPhysChem*, 2012, **13**, 3092-3097.
5 R. A. Sperling, P. R. Gil, F. Zhang, M. Zanella and W. J. Parak, *Chem. Soc. Rev.*, 2008, **37**, 1896-1908.
6 S. Kumar, N. Harrison, R. Richards-Kortum and K. Sokolov, *Nano Lett.*, 2007, **7**, 1338-1343.
7 B. Duncan, C. Kim and V. M. Rotello, *J. Control Release*, 2010, **148**, 122-127.
8 M. Haruta, *Chem. Rec.*, 2003, **3**, 75-87.
9 T. Torimoto, K. Okazaki, T. Kiyama, K. Hirahara, N. Tanaka and S. Kuwabata, *Appl. Phys. Lett.*, 2006, **89**, 243117.
10 M. Brust, M. Walker, D. Bethell, D. J. Schiffrin and R. Whyman, *J. Chem. Soc., Chem. Commun.*, 1994, 801-802.
11 S. C. Hamm, S. Basuray, S. Mukherjee, S. Sengupta, J. C. Mathai, G. A. Baker and S. Gangopadhyay, *J. Mater. Chem. A*, 2014, **2**, 792-803.
12 M. S. Sibbald, G. Chumanov and T. M. Cotton, *J. Phys. Chem.*, 1996, **100**, 4672-4678.
13 K. Richter, A. Birkner and A.-V. Mudring, *Phys. Chem. Chem. Phys.*, 2011, **13**, 7136-7141.
14 H. Wender, P. Migowski, A. F. Feil, L. F. de Oliveira, M. H. G. Precht, R. Leal, G. Machado, S. R. Teixeira and J. Dupont, *Phys. Chem. Chem. Phys.*, 2011, **13**, 13552-13557.
15 E. Vanecht, K. Binnemans, J. W. Seo, L. Stappers and J. Fransaer, *Phys. Chem. Chem. Phys.*, 2011, **13**, 13565-13571.
16 Y. Hatakeyama, K. Onishi and K. Nishikawa, *RSC Advances*, 2011, **1**, 1815-1821.
17 D. Sugioka, T. Kameyama, S. Kuwabata and T. Torimoto, *Phys. Chem. Chem. Phys.*, 2015, **17**, 13150-13159.
18 K. Richter, A. Birkner and A.-V. Mudring, *Angew. Chem. Int. Ed.*, 2010, **49**, 2431-2435.
19 V. S. Raghuwanshi, M. Ochmann, A. Hoell, F. Polzer and K. Rademann, *Langmuir*, 2014, **30**, 6038-6046.
20 T. Ienaga, Y. Nakahara and K. Kimura, *Chem. Lett.*, 2014, **43**, 1893-1895.
21 J. Neddersen, G. Chumanov and T. M. Cotton, *Appl. Spectrosc.*, 1993, **47**, 1959-1964.
22 H. Wender, L. F. de Oliveira, A. F. Feil, E. Lissner, P. Migowski, M. R. Meneghetti, S. R. Teixeira and J. Dupont, *Chem. Commun.*, 2010, **46**, 7019-7021.
23 H. Wender, R. V. Goncalves, A. F. Feil, P. Migowski, F. S. Poletto, A. R. Pohlmann, J. Duopnt and S. R. Teixeira, *J. Phys. Chem. C*, 2011, **115**, 16362-16367.
24 Y. Hatakeyama, T. Morita, S. Takahashi, K. Onishi and K. Nishikawa, *J. Phys. Chem. C*, 2011, **115**, 3279-3285.
25 S. Suzuki, T. Suzuki, Y. Tomita, M. Hirano, K. Okazaki, S. Kuwabata and T. Torimoto, *CrystEngComm*, 2012, **14**, 4922-4926.
26 T. Suzuki, K. Okazaki, S. Suzuki, T. Shibayama, S. Kuwabata and T. Torimoto, *Chem. Mater.*, 2010, **22**, 5209-5215.
27 E. F. Borra, O. Seddiki, R. Angel, D. Eisenstein, P. Hickson, K. R. Seddon and S. P. Worden, *Nature*, 2007, **447**, 979-981.
28 E. C. da Silva, M. G. A. da Silva, S. M. P. Meneghetti, G. Machado, M. A. R. C. Alencar, J. M. Hickmann and M. R. Meneghetti, *J. Nanopart. Res.*, 2008, **10**, 201-208.
29 N. Wu, L. Fu, M. Su, M. Aslam, K. C. Wong and V. P. Dravid, *Nano Lett.*, 2004, **4**, 383-386.
30 S. Gyergyek, D. Makovec and M. Drofenik, *J. Colloid Interface Sci.*, 2011, **354**, 498-505.
31 M. D. Abramoff, P. J. Magalhaes and S. J. Ram, *Biophotonics International*, 2004, **11**, 36-42.
32 Y. Hatakeyama, M. Okamoto, T. Torimoto, S. Kuwabata, K. Nishikawa, J. Phys. Chem. C, 2009, 113, 3917-3922.
33 A. P. Hammersley, S. O. Svensson, M. Hanfland, A. N. Fitch and D. Häusermann *High Pressure Res.*, 1996, **14**, 235-248.
34 E. Vanecht, K. Binnemans, S. Patskovsky, M. Meunier, J. W. Seo, L. Stappers, and J. Fransaer, *Phys. Chem. Chem. Phys.* 2012, **14**, 5662-5671.
35 T. Laaksonen, P. Ahonen, C. Johans and K. Kontturi, *ChemPhysChem*, 2006, **7**, 2143-2149.
36 B. Hu, X. Cao and P. Zhang, *ChemPlusChem* 2013, **78**, 506-514.
37 M. D. Scanlon, P. Peljo, M. A. Méndez, E. Smirnov and H. H. Girault, *Chem. Sci.*, 2015, **6**, 2705-2720.
38 C. Novo, A. M. Funston, and P. Mulvaney, *Nature Nanotech.*, 2008, **3**, 598-602.
39 T. Ung, M. Giersig, D. Dunstan and P. Mulvaney, *Langmuir*, 1997, **13**, 1773-1782.

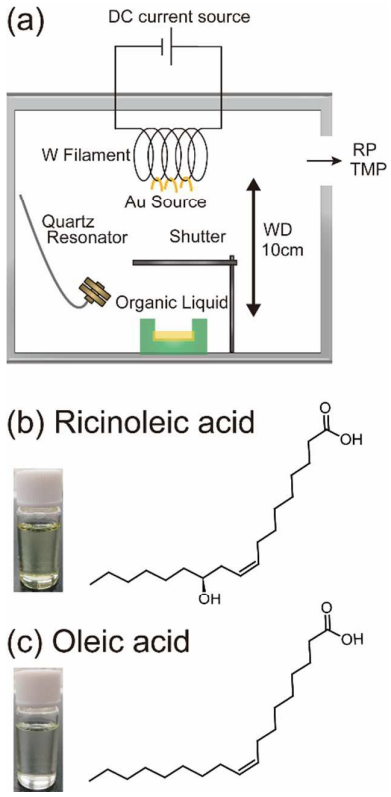

Fig. 1 (a) A schematic illustration of the experimental apparatus and (b), (c) structural formulas with photographs of ricinoleic and oleic acids. Both UFAs are transparent and ricinoleic acid has a light yellow color while oleic acid is colorless.

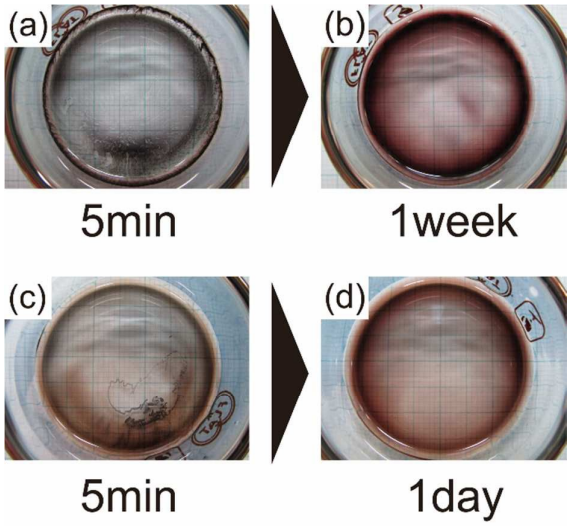

Fig. 2 Time-dependent photographs of UFAs. The photographs were taken (a) 5 minutes and (b) 1 week after deposition in ricinoleic acid and (c) 5 minutes and (d) 1 day after deposition in oleic acid. At 5 minutes after deposition, black aggregates were observed on the surface and inside the solvent in ricinoleic acid, while most of the aggregates seemed on the surface in oleic acid. At 1 week after deposition, both UFAs presented a homogenous color. All photographs of the samples were taken on a cross-section paper.

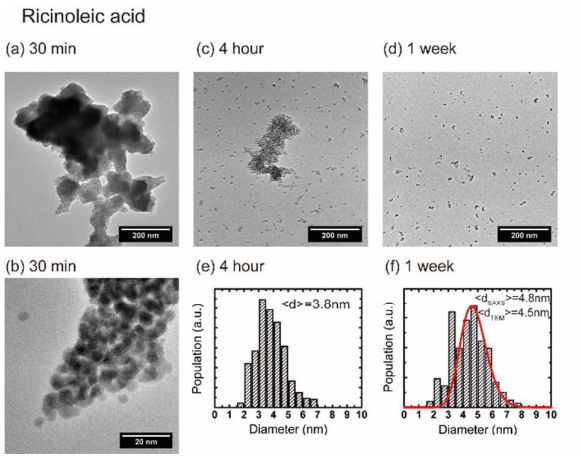

Fig. 3 TEM pictures of the gold nanoparticles formed in ricinoleic acid. The photographs (a), (c) and (e) are typical TEM pictures taken 30 minutes, 4 hours and 1 week after deposition, respectively. The magnification were set to 30k times. The photograph (b) shows a 300k times magnification TEM picture of the same aggregate (a). Aggregates in the size of several microns were observed and the aggregates were composed of nanoparticles in the size of several nanometers. The graphs (e) and (f) display the size distribution derived from (c) and (d). Size distributions could not be obtained from (a) since individual nanoparticles were scarce. The red line shown in (f) stand for the size distribution obtained from SAXS measurements. Scattering profiles are presented in the ESI.

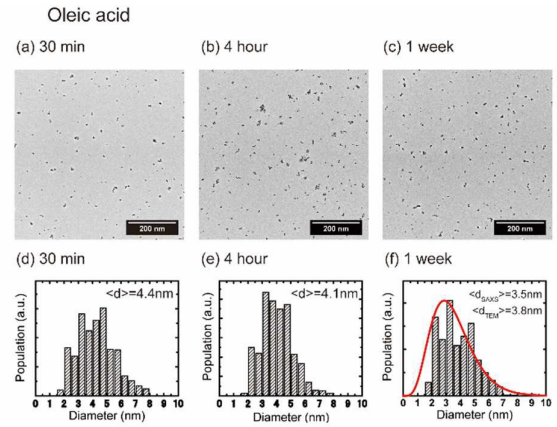

Fig. 4 TEM pictures of the gold nanoparticles formed in oleic acid. The photographs (a), (c) and (e) are typical TEM pictures taken 30 minutes, 4 hours and 1 week after deposition, respectively. The magnification were set to 30k times. Huge aggregates in the size of several microns were not observed as in ricinoleic acid and the nanoparticles were mostly dispersed in all TEM pictures. The graphs (d), (e) and (f) display the size distribution derived from (a), (b) and (c), respectively. The red line shown in Fig. 3(f) stands for the size distribution obtained from SAXS measurements. Scattering profiles are presented in the ESI.

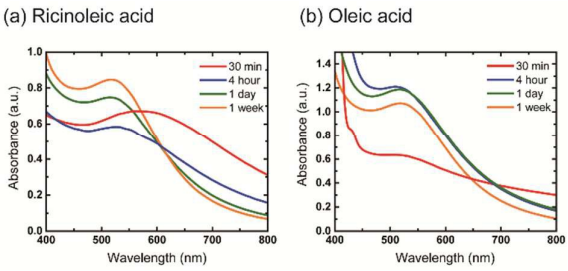

Fig. 5 Absorption spectra of both solvents as a function of time for (a) ricinoleic acid and (b) oleic acid. In ricinoleic acid, a broad peak around 600 nm was observed and then shifted to around 520 nm after 4 hours of deposition. This reflects the transfer from an aggregate to individual nanoparticles. In oleic acid, a clear peak cannot be confirmed 30 minutes after deposition. A peak around 520 nm was observed after 4 hours of deposition, reflecting the transfer from thin films to nanoparticles.

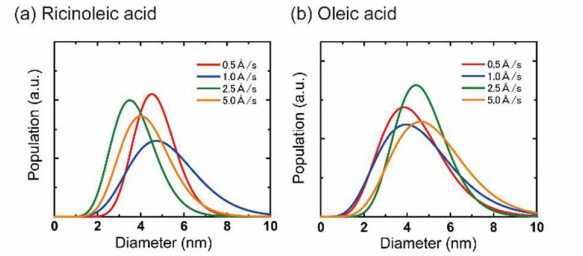

Fig. 6 Size distribution of gold nanoparticles synthesized in (a) ricinoleic and (b) oleic acid, obtained by SAXS measurements. Deposition rates were changed from 0.5 Å/s to 5.0 Å/s. Clear correlations between the deposition rate and size distribution could not be recognized.

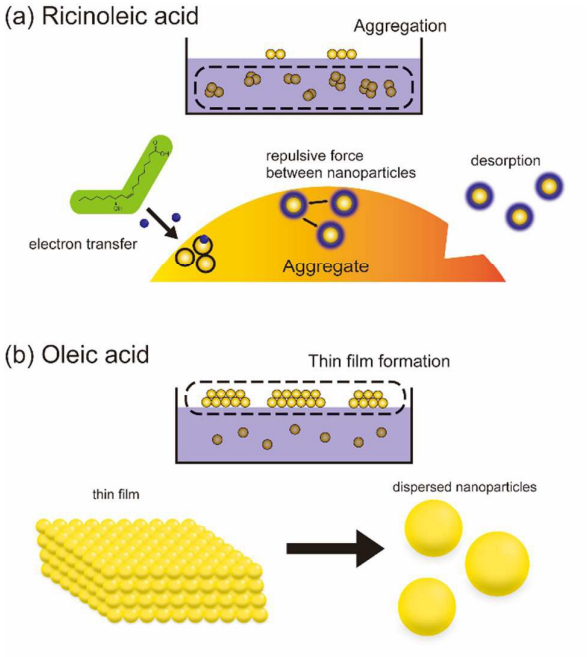

Fig. 7 Schematic illustration of the behavior of the aggregates (a) in the solvent and (b) on the surface. The navy spheres represent electrons. (a) and (b) were mainly observed in ricinoleic and oleic acid, respectively. (a) UFA molecules get oxidized and electrons were transferred to the surface of the aggregate. The nanoparticles positioned on the surface get negatively charged and repulsive forces arise between them. Further electron transfer causes desorption of the nanoparticles from the aggregate. (b) Crystalline thin films form on the UFA after deposition. The films become stimulated by the electrons induced by the oxidation of the UFA and diffuse into the solvent changing into nanoparticles.